Glassy Dynamics, Spinodal Fluctuations, and the Kinetic Limit of Nucleation in Suspensions of Colloidal Hard Rods

Ran Ni,[1] Simone Belli,[2] René van Roij,[2] and Marjolein Dijkstra[1]

[1]*Soft Condensed Matter, Utrecht University, Princetonplein 5, 3584 CC Utrecht, The Netherlands*

[2]*Institute for Theoretical Physics, Utrecht University, Leuvenlaan 4, 3584 CE Utrecht, The Netherlands*

(Received 23 March 2010; published 16 August 2010)

Using simulations we identify three dynamic regimes in supersaturated isotropic fluid states of short hard rods: (i) for moderate supersaturations, we observe nucleation of multilayered crystalline clusters; (ii) at higher supersaturation, we find nucleation of small crystallites which arrange into long-lived locally favored structures that get kinetically arrested; and (iii) at even higher supersaturation, the dynamic arrest is due to the conventional cage-trapping glass transition. For longer rods we find that the formation of the (stable) smectic phase out of a supersaturated isotropic state is strongly suppressed by an isotropic-nematic spinodal instability that causes huge spinodal-like orientation fluctuations with nematic clusters diverging in size. Our results show that glassy dynamics and spinodal instabilities set kinetic limits to nucleation in highly supersaturated hard-rod fluids.

DOI: 10.1103/PhysRevLett.105.088302 PACS numbers: 82.70.Dd, 68.55.A−, 82.60.Nh

Nucleation is the process whereby a thermodynamically metastable state evolves into a stable one, via the spontaneous formation of a droplet of the stable phase. From classical nucleation theory (CNT), the Gibbs free energy associated with the formation of a spherical cluster of the stable phase with radius R in the metastable phase is given by $\Delta G = -4\pi R^3 \rho |\Delta\mu|/3 + 4\pi R^2 \gamma$, with γ the surface tension between the coexisting phases, ρ the density of the cluster, and $|\Delta\mu| > 0$ the chemical potential difference between the metastable and stable phase. CNT predicts a nucleation barrier $\Delta G_{\rm crit} = (16\pi/3)\gamma^3/(\rho|\Delta\mu|)^2$ and a critical nucleus radius $R_{\rm crit} = 2\gamma/\rho|\Delta\mu|$. CNT predicts an infinite barrier at bulk coexistence ($\Delta\mu = 0$), which decreases with increasing supersaturation. However, CNT incorrectly predicts a *finite* barrier at the spinodal, whereas a nonclassical approach yields a vanishing barrier at the spinodal, with a diffuse critical nucleus that becomes of infinite size [1]. Both approaches explain why liquids must be supercooled substantially before nucleation occurs, and one might expect that nucleation should always occur for sufficiently high supersaturation. For deep quenches of soft spheres close to a spinodal, but not beyond it, simulation studies show either nucleating anisotropic and diffuse clusters or precritical clusters that grow further or that coalesce in ramified structures [2]. These results contrast the mean-field predictions that the critical size should diverge at the spinodal [1]. Wedekind *et al.* showed that a Lennard-Jones system can become unstable by a so-called kinetic spinodal, where the largest cluster in the system has a vanishing barrier, i.e., $\Delta G_{\rm crit}^{\rm large} = 0$, implying the immediate formation of a critical cluster in the system [3]. Beyond this kinetic limit, which is system-size-dependent as $\Delta G_{\rm crit}^{\rm large} = \Delta G_{\rm crit} - k_B T \ln N$, the system is kinetically unstable, and the phase transformation proceeds immediately via growth of the largest cluster. Here N is the number of particles, k_B the Boltzmann constant, and T the temperature. This scenario also explains why it is hard to reach the thermodynamic spinodal and why a divergence of the critical cluster size is never observed in simulations, as the system already becomes kinetically unstable at much lower supersaturations. Interestingly, recent simulations of silica also showed a kinetic limit of the homogeneous nucleation regime that is strongly influenced by glassy dynamics, without any spinodal effects [4]. Clearly, the nucleation kinetics at high supersaturation is still poorly understood.

In this Letter, we investigate the nucleation pathways of the isotropic-crystal (IX) transition of rodlike particles as a function of supersaturation and those of the isotropic-smectic (ISm) transition. The nucleation pathways of structures with both orientational and positional order are still unknown, as nucleating smectic or crystalline clusters have never been observed in experiments or simulations [5,6]. We show for the first time that IX nucleation proceeds via multilayer nuclei, while previous studies found that nucleation is hampered by self-poisoning [5]. Additionally, we identify two mechanisms of dynamic arrest that set a kinetic limit to the IX nucleation regime, one based on dynamic arrest of small crystalline nuclei that form locally favored structures and one based on a conventional cage-trapping glass transition. Moreover, for longer rods we show that the isotropic-nematic (IN) spinodal associated with a metastable IN transition severely hinders and even prevents ISm nucleation.

We consider a suspension of N hard spherocylinders with a diameter σ and a cylindrical segment of length $L = 2\sigma$ in a volume V or at pressure P. The bulk phase diagram of these rods with a length-to-diameter ratio $L^* = L/\sigma = 2$ is well known [7]; it features an IX transition at pressure $P^* = \beta P \sigma^3 = 5.64$, with $\beta = 1/k_B T$.

We first use *NPT* Monte Carlo (MC) simulations to compress an isotropic fluid of 10 000 rods at the moderate pressure $P^* = 7.6$ corresponding to a chemical potential

difference $\beta|\Delta\mu| = 1.11$ between the (metastable) fluid and the crystal phase. We then take random MC configurations as initial configurations for molecular dynamics (MD) simulations in the *NVT* ensemble to study spontaneous crystal nucleation, employing the cluster criterion as described in Refs. [8,9]. We find spontaneous nucleation of a multilayered crystalline cluster in the isotropic fluid. Figure 1(a) shows the time evolution from a typical MD trajectory. In the initial stage of the MD simulation, the system remains in the metastable isotropic fluid for a long time. After time $t = 1000\tau$, with $\tau = \sigma\sqrt{m/k_BT}$ and m the mass of the particle, a nucleus consisting of multiple crystalline layers starts to grow gradually until the whole system has been transformed into the bulk crystal phase. We note that the cluster prefers to grow laterally as was also found for attractive rods [6]. We observed similar spontaneous nucleation at $P^* = 7.4$. The long waiting time t_w before a postcritical cluster appears by a spontaneous fluctuation is typical for nucleation and growth. We calculate the nucleation rate $R = 1/\langle t_w\rangle V$ and find from MD simulations that $R\sigma^3\tau = 5 \times 10^{-9\pm2}$ and $1.7 \times 10^{-8\pm1}$, for $P^* = 7.4$ and 7.6, respectively.

As our MD simulations provide evidence that the IX transformation can occur via nucleation of multilayer crystalline clusters, we determine the nucleation barrier by using umbrella sampling (US) in MC simulations [8]. We perform MC simulations of 2000 particles at $P^* = 7.0$, 7.2, and 7.4 corresponding to $\beta|\Delta\mu| = 0.78$, 0.89, and 1.0, respectively. Figure 1(b) shows $\Delta G(n)$, which for $P^* = 7.2$ and 7.4 displays a maximum of $\beta\Delta G_{\rm crit} \approx 27 \pm 1.5$ and 20 ± 1.5 at critical cluster sizes $n_{\rm crit} \approx 140$ and 80, respectively. A typical configuration of the critical cluster, consisting of three crystalline layers at $P^* = 7.4$, is shown in the inset in Fig. 1(b); its structure agrees with those observed in our MD simulations of spontaneous nucleation of multilayer crystallites. For $P^* = 7.0$ the free-energy barrier is too high to be calculated in our simulations as the cluster starts to percolate the simulation box before the top is reached. For lower pressures, i.e., $P^* = 6.0$ (not shown), this problem is even more severe. For clusters up to $n \simeq 100$, the barrier can be calculated with the US scheme, revealing multilayered structures very similar to the one shown for $P^* = 7.4$. Our MC simulation results for $P^* = 7.2$ and 7.4 can also be used to calculate the nucleation rate from $R = \kappa\exp(-\beta\Delta G_{\rm crit})$ with kinetic prefactor $\kappa = |\beta\Delta G''_{\rm crit}/(2\pi)|^{1/2}\rho_{\rm I} f_{n_{\rm crit}}$, with $\rho_{\rm I}$ the number density of the isotropic fluid and $f_{n_{\rm crit}}$ the attachment rate of particles to the critical cluster (which we compute by using MD simulations starting with independent configurations at the top of the nucleation barrier [10]). For $P^* = 7.2$ and 7.4 we find $R\sigma^3\tau = 1 \times 10^{-13\pm1}$ and $2 \times 10^{-10\pm1}$, respectively, in agreement within error bars with the MD simulations.

Our observation of bulk crystal nucleation of short rods is in marked contrast with an earlier study, which showed that the free energy never crosses a nucleation barrier [5]. These simulations showed the formation of a single crystalline layer, while subsequent crystal growth is hampered. The authors attributed the stunted growth of this monolayer to self-poisoning by rods that lie flat on the cluster surface. If we use the same cluster criterion as in Ref. [5] for the biasing potential, we indeed find crystalline monolayers at $P^* = 7.4$, which cannot grow further as $\Delta G(n)$ increases monotonically with n. These results for the nucleation barrier agree with theoretical predictions that for sufficiently low supersaturations $\Delta G(n)$ for a single layer is always positive, while multilayer crystalline clusters can grow spontaneously when the nucleus exceeds the critical size [11]. However, our detailed check [9] of the order parameter in Ref. [5] actually reveals a strong (unwanted) bias to form single-layered clusters in US simulations.

We also study the IX transformation at higher supersaturation. To this end, we compress 1000 rods ($L^* = 2$) in *NPT*-MC simulations at $P^* = 8$ ($\beta|\Delta\mu| = 1.33$). Using $\beta\gamma\sigma^2 \simeq 0.44$, which follows from fitting the two barriers of Fig. 1(b) to CNT, we estimate barriers as low as $\beta\Delta G_{\rm crit} \sim 12$ and $\beta\Delta G^{\rm large}_{\rm crit} \sim 5$ for $P^* = 8$. Indeed, many small crystallites nucleate immediately after the compression quench, indicative of the proximity of a kinetic spinodal. These crystallites are oriented in different directions and have a large tendency to orient perpendicular to each other. The subsequent equilibration is extremely

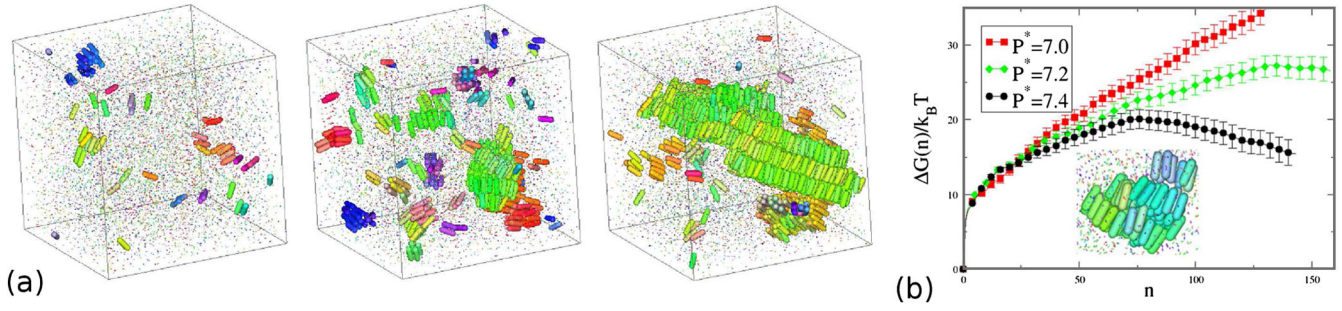

FIG. 1 (color online). (a) Configurations for spontaneous crystal nucleation from a typical molecular dynamics trajectory at $P^* = 7.6$ and $t/\tau = 0$, 1000, and 3000 (from left to right). Isotropiclike particles are drawn 10 times smaller than their actual size. A movie can be found in Ref. [9]. (b) Gibbs free energy $\Delta G(n)$ as a function of the number of rods n in the crystalline cluster at pressure $P^* = 7.0$, 7.2, and 7.4. Inset: A typical configuration of a critical cluster ($n = 81$) at $P^* = 7.4$.

slow, since the growth of a single crystal evolves via collective rearrangements of smaller clusters that subsequently coalesce. In fact, after 3×10^7 MC cycles, our system is dynamically arrested. Interestingly, Frank proposed more than 50 years ago that dynamic arrest may be attributed to the formation of *locally favored structures* (LFS) in which the system gets kinetically trapped in local potential-energy minima [12], while direct observation of such a mechanism for dynamic arrest was only recently reported in the gel phase of a colloid-polymer mixture [13]. In our simulations, we clearly observe the formation of long-lived LFS consisting of perpendicularly oriented crystallites. Only via cooperative rearrangements (rotation of the whole cluster) can the system escape from the kinetic traps, but these events are rare in MC simulations. So, despite the large supersaturation and the low barrier as predicted by CNT, the actual formation of a single crystal is impeded dramatically by slow dynamics. Our observations agree with experiments on soft-repulsive selenium rods, where transient structures of 5–10 aligned particles tend to form LFS with perpendicularly oriented clusters, which gradually merge into larger clusters [14].

To investigate whether the system can be quenched *beyond* a thermodynamic spinodal (such that the transformation proceeds via spinodal decomposition), we perform simulations at $P^* = 10$. We find again the immediate nucleation of many small crystallites, as expected beyond the kinetic spinodal. As the phase transformation sets in right away, we cannot determine whether the nucleation barrier is finite or zero; it is therefore unclear whether or not we have crossed a thermodynamic spinodal (if there is one for freezing). However, we did not find any characteristics of early-stage spinodal decomposition. The small crystallites tend to orient perpendicularly, and the system displays clear orientational ordering along three perpendicular directions (cubatic order), as shown by the orientation distribution on the surface of a unit sphere in the inset

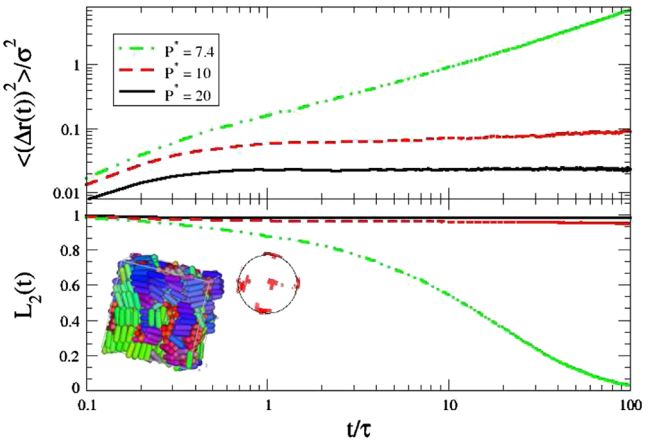

FIG. 2 (color online). Mean-square displacement $\langle[\Delta\mathbf{r}(t)]^2\rangle$ and second-order orientational correlator $L_2(t)$ for hard rods with $L^* = 2$ and pressures as labeled. The inset shows a typical configuration of a glassy state with cubatic order at $P^* = 10$.

in Fig. 2. To check for finite size effects, we studied a system of $N = 4000$ rods, which again shows system-spanning cubatic order. Whether or not the cubatic order is long-ranged for even larger systems remains unsettled. The mean-square displacement $\langle[\Delta\mathbf{r}(t)]^2\rangle$ and the second-order orientational correlator $L_2(t) = \langle[3\cos^2\theta(t) - 1]/2\rangle$ are displayed in Fig. 2, which shows the characteristic plateau of structural arrest. For comparison, we also present data for $P^* = 7.4$, which show relatively fast relaxation of the translational and orientational degrees of freedom. At an even larger supersaturation $P^* = 20$, we find that the system is kinetically arrested immediately after the quench. We find hardly any crystalline order, while the orientation distribution remains isotropic (not shown). Clearly, the system crossed the conventional cage-trapping glass transition [15] that prevents the formation of any ordering. The dynamic arrest can be appreciated by the plateau in $\langle[\Delta\mathbf{r}(t)]^2\rangle$ and $L_2(t)$ in Fig. 2. Our results thus show that nucleation at high supersaturation is strongly affected by vitrification, either due to LFS or by the conventional glass transition, yielding glasses with and without small crystallites, respectively.

We also study longer hard rods with $L^* = 3.4$, which show ISm coexistence at $P^* = 2.828$. A previous MC simulation study [16] showed the formation of the smectic phase out of the highly supersaturated I phase at $P^* = 3.1$ via spinodal decomposition. However, nucleation and growth of the smectic phase out of weakly supersaturated I phases at $P^* = 2.85$–3.0 was *not* observed [16]. As strong presmectic ordering and huge nematiclike clusters were observed in the I phase, the hampered nucleation was attributed to slow dynamics. Here we reinvestigate the regime $P^* = 2.828$–3.0 at much longer time scales by MD simulations. We confirm the earlier findings of the structure but do not find any evidence for structural arrest in $\langle[\Delta\mathbf{r}(t)]^2\rangle$ and $L_2(t)$ (not shown). Instead, we find huge and strongly fluctuating nematiclike clusters [9]. The nematic character of the clusters is evident from the structure factor $S(k)$ and orientational structure factor $S_{or}(k)$, shown in Fig. 3, revealing a small-k divergence for $S_{or}(k)$ but not for $S(k)$ [15]. The correlation length ξ of the orientational fluctuations obtained from fitting the orientational correlation function $g_{or}(r) \sim \exp(-r/\xi)/r$ is shown in the inset to satisfy a power law $\xi \sim |P - P_c|^{-\nu}$, with $P_c^* = 3.01$ the alleged IN-spinodal pressure and $\nu = 0.47$, which is close to the expected mean-field exponent $\nu = 1/2$ of the IN spinodal [17]. Apparently, the ISm nucleation is prevented by an intervening IN spinodal. Our observation that the metastable isotropic fluid is more susceptible to nematic than to smectic fluctuations is corroborated by second-virial calculations of the Zwanzig model of blocklike $H \times D \times D$ rods with three orthogonal orientations [9]. The dimensionless Helmholtz free-energy density F/V of the I, N, and Sm phases for $H/D = 4.3$, shown in Fig. 3, reveal equilibrium ISm coexistence and a metastable N branch. The IN spinodal on the metastable isotropic branch occurs at a lower packing fraction η than the ISm spinodal. In

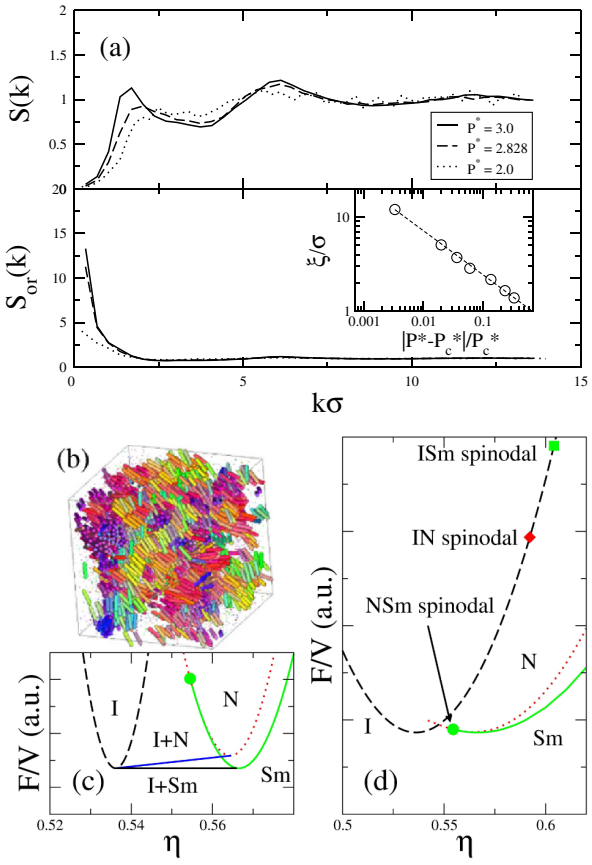

FIG. 3 (color online). (a) Positional (top) and orientational (bottom) structure factor of hard rods with $L/\sigma = 3.4$ at varying P^*. The inset shows the pressure dependence of the orientation correlation length ξ. The dashed line is the power-law fitting $\xi \sim |P - P_c|^{-\nu}$. (b) Typical configuration at $P^* = 3$. A movie is shown in Ref. [9]. Isotropiclike particles are drawn 10 times smaller than their actual size. (c),(d) Conveniently shifted and scaled Helmholtz free-energy density F/V of Zwanzig rods (packing fraction η, aspect ratio $H/D = 4.3$) in the I (dashed), N (dotted), and Sm (green) phases. ISm and metastable IN coexistence are indicated by the solid lines, and the IN and ISm spinodal instabilities are denoted by the symbols on the supersaturated isotropic free-energy branch.

other words, the isotropic fluid is predicted to exhibit spinodal nematic fluctuations upon increasing the supersaturation, consistent with the diverging ξ as observed in our simulations. One might expect that the presence of these nematic clusters facilitates the formation of the smectic phase. However, although we find some layering of the rods, the density within these nematic clusters is too low and the orientational fluctuations change too rapidly to form the smectic layers.

In conclusion, our results show that nucleation of hard rods from a supersaturated isotropic fluid phase to crystal and smectic phases is much more rare than perhaps naively anticipated. Only for very short rods and moderate supersaturations do we find nucleation of multilayered crystals; at higher supersaturations, we identified two mechanism for dynamic arrest. The first one occurs close to the kinetic spinodal, where (locally favored) crystalline clusters appear immediately after the quench, followed by slow dynamics due to geometric constraints of these tightly packed clusters. The second type of dynamic arrest occurs at very high supersaturation and is due to the conventional cage-trapping glass transition. In the supersaturated isotropic state of longer rods ($L^* = 3.4$), the nucleation of the (equilibrium) smectic phase is found to be hampered by nematic fluctuations due to the existence of an IN-spinodal instability. We showed for the first time that for quenches close to a spinodal the clusters diverge in size. Our findings are of fundamental and practical interest. They provide strong evidence for a local structural mechanism for dynamic arrest in a system with orientational and positional degrees of freedom. They also explain why the self-organization of ordered assemblies of nanorods is difficult and why most of the nanorod self-assembly techniques require additional alignment of the rods by applied electric fields, fluid flow, or substrates in order to facilitate the formation of the desired self-assembled structures [18]. Our simulations show that this additional "steering" is required since the spontaneous nucleation of the rods is strongly affected by glassy dynamics and spinodal instabilities.

Financial support of a NWO-VICI grant is acknowledged. This work is part of the research program of FOM, which is financially supported by NWO.

[1] K. Binder, Phys. Rev. A **29**, 341 (1984).
[2] H. Wang, H. Gould, and W. Klein, Phys. Rev. E **76**, 031604 (2007); F. Trudu, D. Donadio, and M. Parrinello, Phys. Rev. Lett. **97**, 105701 (2006); P. Bhimalapuran, S. Chakrabarty, and B. Bagchi, Phys. Rev. Lett. **98**, 206104 (2007).
[3] J. Wedekind *et al.*, J. Chem. Phys. **131**, 114506 (2009).
[4] I. Saika-Voivod, R. K. Bowles, and P. H. Poole, Phys. Rev. Lett. **103**, 225701 (2009).
[5] T. Schilling and D. Frenkel, Phys. Rev. Lett. **92**, 085505 (2004).
[6] A. Patti and M. Dijkstra, Phys. Rev. Lett. **102**, 128301 (2009).
[7] P. Bolhuis *et al.*, J. Chem. Phys. **106**, 666 (1997).
[8] A. Cuetos and M. Dijkstra, Phys. Rev. Lett. **98**, 095701 (2007).
[9] See supplementary material at http://link.aps.org/supplemental/10.1103/PhysRevLett.105.088302 for movies and technical details.
[10] S. Auer *et al.*, Nature (London) **409**, 1020 (2001).
[11] D. Frenkel and T. Schilling, Phys. Rev. E **66**, 041606 (2002).
[12] F. C. Frank, Proc. R. Soc. A **215**, 43 (1952).
[13] C. P. Royall *et al.*, Nature Mater. **7**, 556 (2008).
[14] H. Maeda and Y. Maeda, Phys. Rev. Lett. **90**, 018303 (2003).
[15] M. Letz and A. Latz, Phys. Rev. E **60**, 5865 (1999).
[16] A. Cuetos *et al.*, Faraday Discuss. **144**, 253 (2010).
[17] E. F. Gramsbergen *et al.*, Phys. Rep. **135**, 195 (1986).
[18] D. Baranov *et al.*, Nano Lett. **10**, 743 (2010).